

Self-calibrating binary polarization analyzer

X. Steve Yao

Optical Polarization Research Center, Tianjin University, Tianjin, China, and General Photonics Corporation, 5228 Edison Avenue, Chino, California 91710

Xiaojun Chen and Lianshan Yan

General Photonics Corporation, 5228 Edison Avenue, Chino, California 91710

Received February 13, 2006; accepted April 7, 2006; posted April 24, 2006 (Doc. ID 68011)

We report a self-calibrating polarization analyzer fabricated with binary magneto-optic polarization rotators. The device automatically overcomes wavelength and temperature dependent inaccuracies and has impressive state of polarization and degree of polarization accuracies of 0.3° and $\pm 0.5\%$, respectively, from 1460 to 1580 nm. © 2006 Optical Society of America

OCIS codes: 120.5410, 080.2730, 060.2300, 260.5430.

Accurate optical polarization analysis for various applications has been an active topic of research for the past 30 years.¹⁻⁷ In a previous publication,⁸ we reported a magneto-optic (MO) polarization-state generator (PSG) for generating 5 or 6 distinctive polarization-states across the Poincaré sphere with a high repeatability of better than 0.1° . We pointed out in Refs. 8 and 9 that the same device can also function as a polarization-state analyzer (PSA). In this Letter, we describe in detail the operation of such a polarization analyzer and show that it is highly accurate due to the binary high repeatability of the MO crystals. To overcome the wavelength and temperature dependences of the optical components used inside the device, we developed a self-calibrating methodology to automatically extract the effects of wavelength and temperature variations on measurement accuracy. With the device, we achieved a remarkable degree of polarization (DOP) accuracy of $\pm 0.5\%$, a state of polarization (SOP) accuracy of better than 1.3% , and angular accuracy and resolution of 0.3° and 0.02° , respectively, from 1460 to 1580 nm. This binary MO PSA has the attractive features of low cost, compact size, high repeatability, no moving parts, no wavelength and temperature dependence, and no need for calibration. The device is ideal for low-cost and high-accuracy polarization analysis, system signal-to-noise ratio monitoring,⁹ and accurate measurements of polarization mode dispersion, polarization-dependent loss,³ birefringence, and material properties of thin films^{5,10} when paired with a PSG as described in Ref. 8.

The binary MO PSA is composed of nine or seven functional components: a quarter-wave plate (QWP), two MO rotators before the QWP, four or two MO rotators after the QWP, a polarizer P, and a photodetector, as shown in Fig. 1.

Our MO rotators have the following attractive binary properties⁸: a highly repeatable SOP rotation angle around 22.5° or -22.5° can be obtained with each rotator by applying either a positive or negative magnetic field above a saturation field. Therefore, when two rotators rotate in the same direction, the net rotation is $+45^\circ$ or -45° . On the other hand, if the

two rotators rotate in the opposite direction, the net SOP rotation is zero.

The output power of the PSA can be calculated by multiplying the Mueller matrices of all components in Fig. 1:

$$I_{\text{out}}(\alpha, \beta) = 0.5 \times \{S_0 + [\cos 2\alpha \cos 2(\beta - \theta_p) - \sin 2\alpha \sin 2(\beta - \theta_p) \cos \Gamma] S_1 - [\sin 2\alpha \cos 2(\beta - \theta_p) + \cos 2\alpha \sin 2(\beta - \theta_p) \cos \Gamma] S_2 - [\sin 2(\beta - \theta_p) \sin \Gamma] S_3\}, \quad (1)$$

where θ_p is the relative orientation angle between the QWP and the polarizer, $\Gamma(\lambda)$ is the retardation of the QWP, (S_0, S_1, S_2, S_3) are the Stokes parameters of the input SOP, α is the net rotation angle of the two MO rotators before the QWP, and β is the net rotation angle of the MO rotators after the QWP. α, β can be expressed as

$$\alpha = \sum_{n=1}^2 -(-1)^{bn} \theta, \quad \beta = \sum_{n=3}^6 -(-1)^{bn} \theta, \quad (2)$$

where

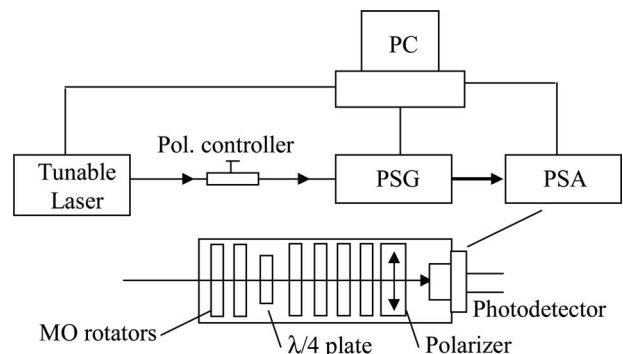


Fig. 1. Schematic of a binary MO PSA and experiment setup. Light exits a PSG and enters a PSA in free space. A high-accuracy reference PSA is put in the place of the PSA under test for comparison.

Table 1. α , β and Logic States of a 6-bit PSA

| I_i | α | β | DLS | I_i | α | β | DLS |
|-------|------------|------------|-----|----------|------------|-----------|-----|
| I_1 | -2θ | -4θ | 1 | I_9 | 2θ | 0 | 1 |
| I_2 | 0 | -4θ | 2 | I_{10} | -2θ | 2θ | 6 |
| I_3 | 2θ | -4θ | 3 | I_{11} | 0 | 2θ | 6 |
| I_4 | -2θ | -2θ | 4 | I_{12} | 2θ | 2θ | 6 |
| I_5 | 0 | -2θ | 4 | I_{13} | -2θ | 4θ | 1 |
| I_6 | 2θ | -2θ | 4 | I_{14} | 0 | 4θ | 2 |
| I_7 | -2θ | 0 | 3 | I_{15} | 2θ | 4θ | 3 |
| I_8 | 0 | 0 | 5 | | | | |

$$\theta = 22.5 + \Delta\theta_0 + k(\lambda - \lambda_0) \quad (3)$$

is the rotation angle of each MO rotator when a magnetic field above saturation is applied, and b_n is 1 or 0 to represent the binary operation of each MO rotator (θ or $-\theta$ rotation, respectively). In deriving Eqs. (2) and (3), we have assumed that all MO rotators are identical (with the same $\Delta\theta_0$, k , and λ_0) and that each rotator has the same rotation angle in both directions. It should be pointed out that $\Delta\theta_0$, k , and λ_0 are functions of temperature in general.

Because each MO rotator is binary with two rotation angles, I_{out} has 64 possible values for each input SOP for a device with a total of 6 MO rotators and 16 possible values for a device with 4 MO rotators in general. Assuming that the rotators are identical and the rotation angles in both directions are the same, one can readily conclude by inspecting Fig. 1 or Eq. (2) that α only has three possible values (0, 2θ , -2θ) and that β has only five possible values (0, 2θ , 4θ , -2θ , -4θ) for devices with 6 MO rotators (4 rotators after the QWP). Therefore, I_{out} in Eq. (1) has only $3 \times 5 = 15$ different values, as shown in Table 1. The rest are degenerate. Similarly, β has three possible values (0, 2θ , -2θ) for devices with a total of 4 MO rotators (2 after the QWP) and I_{out} has $3 \times 3 = 9$ different values.

Further degeneracy occurs when the MO rotators, the QWP, and the polarizers are perfect, i.e., $\theta = 22.5^\circ$, $\Gamma = \pi/2$, and $\theta_p = 90^\circ$. In this case, I_{out} has only 6 different values for a device with 6 rotators and 5 different values for a device with 4 rotators. Therefore, out of the 15 logic states in Table 1, there are only 6 nondegenerate states for a perfect 6-bit PSA. Even in a nonperfect situation, these 6 states are more distinctive from one another than the rest, which are nearly degenerate. We call these 6 states distinctive logic states (DLSs). Similarly, there are only 5 DLSs for a 4-bit PSA.

Assuming that all the parameters in Eq. (1), namely, θ_p , Γ , $\Delta\theta_0$, k , and λ_0 , are known, the output of PSA for the i th logic state can be rewritten as

$$I_i = (M_{i0} M_{i1} M_{i2} M_{i4})(S_0 S_1 S_2 S_3)^T \quad (i = 1, 2, \dots, 2^N), \quad (4)$$

where N is the total number of rotators and M_{i0} , M_{i1} , M_{i2} , and M_{i3} can be obtained from Eq. (1) for all MO rotation combinations. For calculating four Stokes

parameters of the input light, at least four different equations are required. Therefore, by measuring four output powers (I_a, I_b, I_c, I_d) of four nondegenerate logic states, one obtains

$$\begin{pmatrix} I_a \\ I_b \\ I_c \\ I_d \end{pmatrix} = \begin{pmatrix} 0.5 & M_{a1} & M_{a2} & M_{a3} \\ 0.5 & M_{b1} & M_{b2} & M_{b3} \\ 0.5 & M_{c1} & M_{c2} & M_{c3} \\ 0.5 & M_{d1} & M_{d2} & M_{d3} \end{pmatrix} \begin{pmatrix} S_0 \\ S_1 \\ S_2 \\ S_3 \end{pmatrix} = \mathbf{M} \begin{pmatrix} S_0 \\ S_1 \\ S_2 \\ S_3 \end{pmatrix}. \quad (5)$$

The four Stokes parameters can therefore be obtained by the reverse transform of Eq. (5), and the corresponding DOP can be calculated using

$$\text{DOP} = \sqrt{S_1^2 + S_2^2 + S_3^2} / S_0.$$

The four powers can be selected from the 15 nondegenerate logic states listed in Table 1. For calculation accuracies, the four equations chosen should be as distinctive as possible and therefore should be chosen from the powers of the 6 distinctive logic states defined previously.

The Mueller matrix method described above requires the parameters of all the components inside a PSA to be known at all wavelengths and all temperatures. However, it is extremely time consuming to measure the wavelength and temperature dependences of all the components. Even if the wavelength and temperature dependences are known, it is often difficult to know the exact wavelength and temperature during measurements. To overcome these difficulties, we describe below a self-calibrating methodology to automatically extract the effects of wavelength and temperature variations on measurement accuracy. One may rewrite Eq. (1) as

$$I_i = f[S_0, S_1, S_2, S_3, \alpha_i, \beta_i, \Delta\Gamma(\lambda), \theta_p], \quad (6)$$

where $i = 1, 2, \dots, 2^N$, N is the total amount of rotators in the PSA, and I_i is the output power of PSA for the i th logic states. In practice, we have 15 nondegenerate equations available for the calculation of a 6-bit PSA and 9 for a 4-bit PSA. Rotation angles α and β , Stokes parameters (S_0, S_1, S_2, S_3) of input light, $\Delta\Gamma(\lambda)$ of the QWP, and θ_p of the polarizer can be calculated simultaneously by numerically solving Eq. (6), without the need of knowing wavelength and temperature. This is the basic concept of self-calibration. A method of solving Eq. (6) is basically to numerically search for the optimized values of $S_0, S_1, S_2, S_3, \Delta\theta_0(\lambda, T), \Delta\Gamma(\lambda, T), k(T)$, and θ_p to make $\sum_j (f_j - I_j)^2$ minimum. Note that one should not use only the distinctive states for the calculation because the slight nondegeneracy of the other states actually contains the information on the deviation caused by wavelength and temperature dependences. Using this method, one can obtain not only the Stokes parameters of the input light but also all the component parameters. In fact, the component parameters obtained at different wavelength and temperature can then be used in Mueller matrix method.

We evaluated the performance of multiple PSAs with the experimental setup in Fig. 1. A PSG as described in Ref. 8 was used to generate 6 distinctive

SOPs at different wavelengths and a PSA under test obtains the corresponding Stokes parameters. The results are then compared with those obtained with a commercial high-performance reference PSA, which replaces our PSA in Fig. 1.

The top row and bottom left part of Fig. 2 show some typical measurement results of an input SOP using the self-calibration method, and the bottom right part shows the obtained wavelength dependences of the rotation angle deviation (from 22.5°) of the MO rotators and the retardation Γ of the QWP. The polarizer angle θ_p obtained is 90.38° . Note that θ , Γ , and θ_p are the averages of six measurements using six distinctive input SOPs (LVP, LHP, L-45, L+45, RCP, and LCP). Curve fitting in Fig. 2(d) yields all the parameters in Eq. (3) for the MO rotators: $k = -0.035/\text{nm}$ and $\Delta\theta_0 = -1.359^\circ$. (λ_0 is set at 1550 nm.) In the bottom right part a small relative alignment error between the PSA and the reference PSA was removed.

The relative SOP error can be obtained by comparing the results with those of the commercial reference PSA using $\sigma = [(S'_1 - S_1)^2 + (S'_2 - S_2)^2 + (S'_3 - S_3)^2]^{1/2}$, where S'_i are the Stokes parameters measured using the reference PSA. The DOP accuracies can be obtained by comparing the measurement results with unity because a high extinction ratio

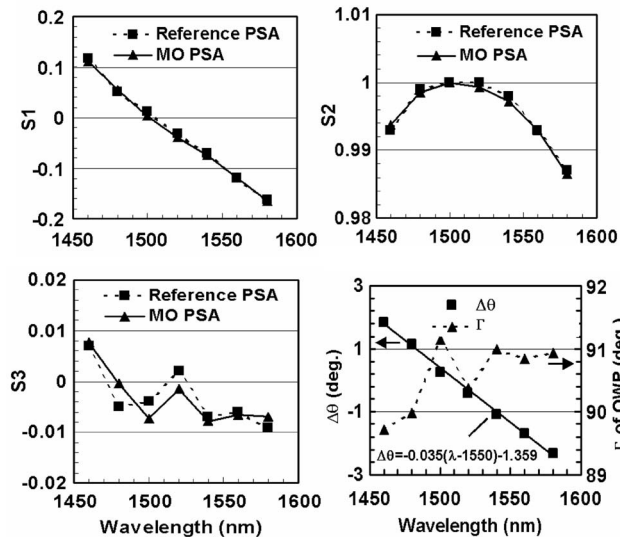


Fig. 2. Experimental results of measured Stokes parameters as a function of wavelength compared with a reference PSA (top left and right, bottom left). The input SOP generated by the PSG is nominally at 45° , linear with a certain wavelength dependence. Bottom right, wavelength dependence of the MO rotators and the QWP inside the PSA, obtained simultaneously using the self-calibration method.

Table 2. Comparison with a Reference PSA (1500–1580 nm)

| Method | Self-cal. | Mueller |
|------------------------|--------------|--------------|
| Max. SOP error | 1.3% | 1.5% |
| Max. DOP error | $\pm 0.35\%$ | $\pm 0.65\%$ |
| DOP standard deviation | 0.28% | 0.4% |

Table 3. Accuracy Measurements with a Polarizer (1460–1580 nm)

| Method | 6-bit | | 4-bit |
|------------------------------------|--------------|---------------|--------------|
| | Self-cal. | Mueller | Self-cal. |
| Angle resolution | 0.02° | $>0.02^\circ$ | 0.02° |
| Max. angle error | 0.30° | 0.27° | 0.34° |
| Standard deviation (SDTV) of angle | 0.12° | 0.09° | 0.12° |
| Max. DOP error | $\pm 0.5\%$ | $\pm 0.75\%$ | $\pm 1.0\%$ |
| DOP average | 0.999 | 0.999 | 1.003 |
| DOP STDV | 0.37% | 0.46% | 0.58% |

(>50 dB) polarizer was placed at the input of the PSG to ensure the DOP of the input light 100%. With both the self-calibration and the Mueller matrix methods (after the component parameters are obtained using the self-calibration method), we characterized multiple 6-bit PSA units at different wavelengths from 1460 to 1580 nm. As shown in Table 2 and Fig. 2, the measurement accuracy remains the same despite the strong wavelength dependences of MO rotation angle θ and QWP retardation Γ .

Note that the measurement errors presented in Table 2 actually include the contributions of PSG fluctuation and the inaccuracy of the reference PSA. To remove these additional uncertainties, we used a polarizer on a precision rotation stage to replace the PSG. Because the input SOP to the PSA is set by the polarizer and is known, the absolute PSA accuracy can be evaluated. As shown in Table 3, the 6-bit PSA has an angular resolution and accuracy of 0.02° and 0.3° , respectively. The DOP accuracy is better than $\pm 0.5\%$ using the self-calibration method. As can be seen, the 6-bit PSA is more accurate than a 4-bit PSA. We took 50 to 100 measurements per SOP state and found that the device has a remarkable repeatability of SOP and DOP of less than 0.3%.

X. S. Yao's e-mail address is syao@generalphotonics.com.

References

1. R. A. Chipman, in *Handbook of Optics*, Vol. II, 2nd ed., M. Bass, ed. (McGraw-Hill, 1995), Chap. 22.
2. D. H. Goldstein and R. A. Chipman, *J. Opt. Soc. Am. A* **7**, 693 (1990).
3. P. A. Williams, *Appl. Opt.* **38**, 6508 (1999).
4. R. Azzam, *Opt. Lett.* **1**, 181 (1977).
5. E. Compain, S. Poirier, and B. Drevillon, *Appl. Opt.*, **38**, 3490 (1999).
6. A. De Martino, Y. K. Kim, E. Garcia-Caurel, B. Laude, and B. Drevillon, *Opt. Lett.* **28**, 616 (2003).
7. S. X. Wang and A. Weiner, *Opt. Lett.* **29**, 923 (2004).
8. X. S. Yao, L. S. Yan, and Y. Q. Shi, *Opt. Lett.* **30**, 1324 (2005).
9. L. S. Yan, X. S. Yao, C. Yu, Y. Wang, L. Lin, Z. Chen, and A. E. Willner, *IEEE Photon. Technol. Lett.* **18**, 643 (2006).
10. D. Goldstein, in *Polarized Light*, 2nd ed. (Marcel Dekker, 2003), Chap. 22.